J. Cent. South Univ. (2015) 22: 214−223
DOI: 10.1007/s11771-015-2512-z

Springer

Serret−Frenet frame based on path following control for underactuated unmanned surface vehicles with dynamic uncertainties

LIAO Yu-lei(廖煜雷)[1], ZHANG Ming-jun(张铭钧)[1, 2], WAN Lei(万磊)[1]

1. Science and Technology on Underwater Vehicle Laboratory, Harbin Engineering University, Harbin 150001, China;
2. College of Mechanical and Electrical Engineering, Harbin Engineering University, Harbin 150001, China

Abstract: The path following problem for an underactuated unmanned surface vehicle (USV) in the Serret−Frenet frame is addressed. The control system takes account of the uncertain influence induced by model perturbation, external disturbance, etc. By introducing the Serret−Frenet frame and global coordinate transformation, the control problem of underactuated system (a nonlinear system with single-input and ternate-output) is transformed into the control problem of actuated system (a single-input and single-output nonlinear system), which simplifies the controller design. A backstepping adaptive sliding mode controller (BADSMC) is proposed based on backstepping design technique, adaptive method and theory of dynamic slide model control (DSMC). Then, it is proven that the state of closed loop system is globally stabilized to the desired configuration with the proposed controller. Simulation results are presented to illustrate the effectiveness of the proposed controller.

Key words: path following; underactuated unmanned surface vehicle; backstepping; dynamic sliding mode control

1 Introduction

Over the past decade, the control problem of underactuated systems has attracted a great deal of attention [1−3]. In this work, we address the path following of underactuated USV with uncertainties. The challenging problem is how to control the ternate freedom motions by only two independent inputs [4]. Recently, path following problem has attracted less attention than trajectory tracking. The USV path following has been addressed with two different methods: one is to treat it as a tracking control [5−7], and the other is to simplify the following control into a regulation problem by adopting proper path following error dynamics equation [8−10]. For the latter method, the Serret−Frenet frame is frequently adopted to obtain the error dynamics equation. ENCARNACAO et al [11] considered a fourth order ship model subjected to constant direction ocean-current disturbance in the Serret−Frenet frame, and developed a control strategy to follow both the straight-line and the circle. In Ref. [12], a path following controller was proposed based on a transformation of the ship kinematics to the Serret−Frenet frame on the path, where an acceleration and linearization of ship dynamics was used. DO and PAN [13] presented an output feedback path following strategy, where ultimate convergence was proven for an underactuated ship with environmental disturbances. However, the proposed method in Ref. [13] requires a state transformation, which becomes singular at some configuration. In Ref. [14], a simplified vessel model was used to develop a path following control system, and a controller was presented based on backstepping technique and Lyapunov's direct method. However, the sway motion is neglected, and the simplified vessel model ignores the influence of nonlinear yaw motion.

Considering the uncertainties of the vehicle model, in Ref. [15], the combined controller of trajectory-tracking and path-following was proposed based on the Lyapunov's direct method, which has obtained good control effect. The problem of combined trajectory-tracking and path-following for underactuated USV with parametric modeling uncertainty was addressed in Ref. [16]. In Ref. [17], a global path following controller was proposed for underactuated ship with non-zero off-diagonal terms. In Ref. [18], the authors assumed that the surge velocity is constant, and proposed a nonsingular Serret−Frenet based path-following controller by Lyapunov's direct method and backstepping technique. However, in the above-mentioned papers the mass and damping matrices of the USVs are presumed to be diagonal. Furthermore, these papers have ignored the impact of the nonlinear damping terms, namely high-

Foundation item: Project(51409061) supported by the National Natural Science Foundation of China; Project(2013M540271) supported by China Postdoctoral Science Foundation; Project(LBH-Z13055) supported by Heilongjiang Postdoctoral Financial Assistance, China; Project (HEUCFD1403) supported by Basic Research Foundation of Central Universities, China
Received date: 2013−09−12; **Accepted date:** 2014−07−08
Corresponding author: LIAO Yu-lei, PhD; Tel: +86−18045623860; E-mail: liaoyulei@hrbeu.edu.cn

speed applications are excluded [19]. It is noted that in Ref. [19], the nonlinear damping matrix is included and DO and PAN proposed a robust path-following method based on backstepping technique and presented experiment results on an USV to illustrate the proposed method. Moreover, DO and PAN [20], the authors considered the influences caused by the non-diagonal term, nonlinear damping and time-varying environmental disturbance, and designed a global robust adaptive path-following controller by using dynamic structure of the ship together with backstepping technique.

In this work, we consider the path following problem for underactuated USV and the limitations of the above paper, and propose a robust control strategy. We develop the path following mathematic model of underactuated USV under the Serret−Frenet frame. Considering the path following problem, a backstepping adaptive dynamical sliding mode controller (BADSMC) is proposed based on backstepping method and theory of dynamical sliding mode control (DSMC). Based on Lyapunov stability analysis, we demonstrate that the original system is globally stabilized in the function of proposed controller. Numerical simulations using the real parameters of a USV are presented to illustrate the effectiveness of our proposed controller, and the advantage of the controller is that control system is strongly robust and adaptive to the parametric modeling uncertainty and environment disturbances.

2 Problem formulation

In this work, the nonlinear damping terms are considered to cover both low-speed and high-speed applications of USV. The frame definitions and motion model of a USV are shown in Fig. 1.

The mathematical model of an underactuated USV moving on a horizontal plane is described as [21]

$$\begin{cases} \dot{x} = u\cos\psi - \upsilon\sin\psi \\ \dot{y} = u\sin\psi + \upsilon\cos\psi \\ \dot{\psi} = r \\ \dot{u} = \dfrac{m_{22}}{m_{11}}\upsilon r - \dfrac{X_u}{m_{11}}u - \dfrac{X_{|u|u}}{m_{11}}|u|u + \dfrac{F_u}{m_{11}} + \dfrac{d_u}{m_{11}} \\ \dot{\upsilon} = -\dfrac{m_{11}}{m_{22}}ur - \dfrac{Y_\upsilon}{m_{22}}\upsilon - \dfrac{Y_{|\upsilon|\upsilon}}{m_{22}}|\upsilon|\upsilon + \dfrac{d_\upsilon}{m_{22}} \\ \dot{r} = \dfrac{m_{11}-m_{22}}{m_{33}}u\upsilon - \dfrac{N_r}{m_{33}}r - \dfrac{N_{|r|r}}{m_{33}}|r|r + \dfrac{T_r}{m_{33}} + \dfrac{d_r}{m_{33}} \end{cases} \tag{1}$$

where x, y and ψ denote the position and orientation of USV in the earth-fixed frame ($\{E\}$-frame); and u, υ, r denote respectively the surge, sway and yaw velocities in the body-fixed frame ($\{B\}$-frame) (see Fig. 1); m_{11}, m_{22}, m_{33} are the vehicle inertial including additional masses;

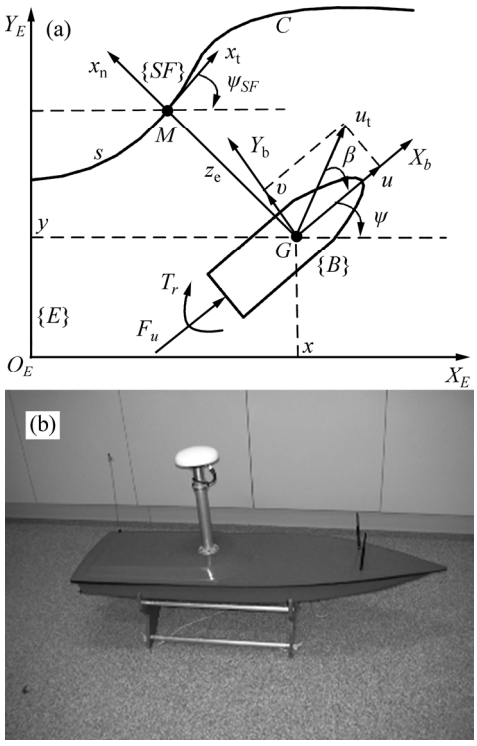

Fig. 1 Underactuated USV model in plane motion: (a) Horizontal plane motion model of USV and frame definitions; (b) A typical USV [19]

$X_u, Y_\upsilon, N_r, X_{|u|u}, Y_{|\upsilon|\upsilon}, N_{|r|r}$ denote the hydrodynamic damping; F_u and T_r; only control inputs are the surge force and yaw moment in $\{B\}$-frame; d_u, d_υ, d_r denote respectively the surge, sway and yaw external disturbances caused by model perturbation, measuring noise, environmental disturbance, which satisfy the bounded condition of $|d_u| \le \bar{d}_u, |d_\upsilon| \le \bar{d}_\upsilon, |d_r| \le \bar{d}_r$, and slow condition of $\dot{d}_u = 0, \dot{d}_\upsilon = 0, \dot{d}_r = 0$.

In the path following problem, we do not consider the speed and time restrictions. Therefore, we assume the surge velocity u is a positive constant (or an independent controller is used to maintain the surge velocity of vehicle). This assumption is applied by many scholars [12, 22]. Hence, the path-following mathematical model of underactuated USV has been simplified into

$$\begin{cases} \dot{x} = u\cos\psi - \upsilon\sin\psi \\ \dot{y} = u\sin\psi + \upsilon\cos\psi \\ \dot{\psi} = r \\ \dot{\upsilon} = -\dfrac{m_{11}}{m_{22}}ur - \dfrac{Y_\upsilon}{m_{22}}\upsilon - \dfrac{Y_{|\upsilon|\upsilon}}{m_{22}}|\upsilon|\upsilon + \dfrac{d_\upsilon}{m_{22}} \\ \dot{r} = \dfrac{m_{11}-m_{22}}{m_{33}}u\upsilon - \dfrac{N_r}{m_{33}}r - \dfrac{N_{|r|r}}{m_{33}}|r|r + \dfrac{T_r}{m_{33}} + \dfrac{d_r}{m_{33}} \\ y_{a1} = x \\ y_{a2} = y \\ y_{a2} = \psi \end{cases} \tag{2}$$

where y_{a1}, y_{a2}, y_{a3} denote the system outputs.

It is clear that Eq. (2) is a nonlinear control system with single-input and ternate-output. The control objective of this work is to propose the yaw moment T_r to drive the USV to follow a desired path C (see Fig. 1), where M is the origin of Serret−Frenet frame ($\{SF\}$-frame), and M is the orthogonal projection of the USV barycenter G on path C. The parameters x_n, x_t denote respectively the normal and tangent unit vectors to the path at M. We define that ψ_{SF} is the angle between x_t and X-axis, the parameter s is the distance along the path C between a arbitrary fixed point in the path and M, and s are bounded and differentiable variable. The parameter z_e denotes the distance between G and M, and $\psi_e=\psi-\psi_{SF}$ denotes cross-track error, the velocity $u_t=\sqrt{u^2+\upsilon^2}$ is total velocity of USV. The β is the angle between u and u_t, i.e., sideslip angle.

Figure 1 shows the diagrammatic sketch of path following under $\{SF\}$-frame. The errors dynamic equation based on $\{SF\}$-frame is developed as follows [12]:

$$\begin{cases}\dot{z}_e=u\sin\psi_e+\upsilon\cos\psi_e\\ \dot{\psi}_e=r-\dfrac{c(s)}{1-c(s)z_e}(u\cos\psi_e-\upsilon\sin\psi_e)\\ \dot{s}=\dfrac{1}{1-c(s)z_e}(u\cos\psi_e-\upsilon\sin\psi_e)\end{cases}\tag{3}$$

where the curvature of the path at point M is denoted by $c(s)$. Note that Eq. (3) is singular when $c(s)z_e=1$. Hence, we consider the following assumptions [13]:

Assumption 1: We assume that the condition $1-c(s)z_e>\lambda^*>0$ is always satisfied.

Assumption 2: The USV parameters satisfy the condition $m_{22}>m_{11}$, and $|m_{22}u_t^2-m_{11}u^2|>0$.

Substituting Eq. (3) into Eq. (2) yields

$$\begin{cases}\dot{z}_e=u_t\sin\psi_e^*\\ \dot{\psi}_e^*=r\left(1-\dfrac{m_{11}u^2}{m_{22}u_t^2}\right)-\dfrac{c(s)u_t\cos\psi_e^*}{1-c(s)z_e}-\\ \qquad\dfrac{u}{u_t^2}\left(\dfrac{Y_\upsilon}{m_{22}}\upsilon+\dfrac{Y_{|\upsilon|\upsilon}}{m_{22}}|\upsilon|\upsilon-\dfrac{d_\upsilon}{m_{22}}\right)\\ \dot{\upsilon}=-\dfrac{m_{11}}{m_{22}}ur-\dfrac{Y_\upsilon}{m_{22}}\upsilon-\dfrac{Y_{|\upsilon|\upsilon}}{m_{22}}|\upsilon|\upsilon+\dfrac{d_\upsilon}{m_{22}}\\ \dot{r}=\dfrac{m_{11}-m_{22}}{m_{33}}u\upsilon-\dfrac{N_r}{m_{33}}r-\dfrac{N_{|r|r}}{m_{33}}|r|r+\dfrac{T_r}{m_{33}}+\dfrac{d_r}{m_{33}}\\ y_1=z_e\\ y_2=\psi_e^*\end{cases}\tag{4}$$

where y_1 and y_2 denote the system outputs; $\psi_e^*=\psi_e+\beta$ is corrected cross-track error [13]. It is obviously that the original Eq. (2) is simplified into Eq. (4) with single-input and twin-output by introducing the Serret−Frenet frame.

Therefore, the control objective can be formally expressed as follows: we consider the path following Eq. (4), and design a feedback control law T_r to ensure the system states (z_e,ψ_e^*) globally stable about the origin.

3 Control design

By the introduction of intermediate controller, backstepping technique makes the controller design procedural and systematical. It is a very effective method of analysis and design for nonlinear system. Hence, backstepping technique is widely applied to nonlinear systems such as the robots, spacecrafts, aircrafts, electric engines, missile, ships [18−25]. In recent years, some researchers have already apply backstepping technique to the control problem of underactuated marine launch systems [26−28].

Before processing the control design, we first ignore the sway external disturbance, i.e. $d_\upsilon=0$. Therefore, the Eq. (4) is rewritten as

$$\begin{cases}\dot{z}_e=u_t\sin\psi_e^*\\ \dot{\psi}_e^*=a_1r+a_2\\ \dot{r}=a_3+\dfrac{T_r}{m_{33}}+\dfrac{d_r}{m_{33}}\\ \dot{\upsilon}=-\dfrac{m_{11}}{m_{22}}ur-\dfrac{Y_\upsilon}{m_{22}}\upsilon-\dfrac{Y_{|\upsilon|\upsilon}}{m_{22}}|\upsilon|\upsilon\\ y_1=z_e\\ y_2=\psi_e^*\end{cases}\tag{5}$$

where $a_1=1-\dfrac{m_{11}u^2}{m_{22}u_t^2}$, $a_3=\dfrac{m_{11}-m_{22}}{m_{33}}u\upsilon-\dfrac{N_r}{m_{33}}r-\dfrac{N_{|r|r}}{m_{33}}|r|r$,

$$a_2=-\frac{c(s)u_t\cos\psi_e^*}{1-c(s)z_e}-\frac{u}{u_t^2}\left(\frac{Y_\upsilon}{m_{22}}\upsilon+\frac{Y_{|\upsilon|\upsilon}}{m_{22}}|\upsilon|\upsilon\right).$$

In the following section, we design the controller for subsystem (z_e,ψ_e^*,r), and prove the sway motion υ is input-to-state stable (ISS).

The sliding mode control (SMC) method has been widely used in nonlinear control systems, but it inevitably contains the "chattering" problem. However, the "chattering" can only be weaken to a certain extent for the SMC. As an effective way to eliminate chattering, DSMC is applied to nonlinear systems such as the arms, robots, nuclear power systems [23−26].

Recently, many scholars have already applied backstepping technique to the control problem of underactuated systems [4, 27−28]. Backstepping technique makes the controller design systematical and procedural. It is a very effective method for sliding mode control for

non-matching uncertainties and non-minimum phase systems [29]. In this work, we propose a BADSMC method by combining backstepping technique with adaptive technology and theory of DSMC.

3.1 State transformation and system analysis

To facilitate the control analysis and design, we consider the following global coordinate transformation:

$$w_{\mathrm{e}}=\psi_{\mathrm{e}}^{*}+\arcsin\left(\frac{kz_{\mathrm{e}}}{\sqrt{1+(kz_{\mathrm{e}})^{2}}}\right) \tag{6}$$

where k is a positive constant.

Substituting Eq. (6) into subsystem (z_e,ψ_e^*,r) of Eq. (5) yields a new system:

$$\begin{cases}\dot{z}_{\mathrm{e}}=u_{\mathrm{t}}\sin\left(w_{\mathrm{e}}-\arcsin\left(\dfrac{kz_{\mathrm{e}}}{\sqrt{1+(kz_{\mathrm{e}})^{2}}}\right)\right)\\ \dot{w}_{\mathrm{e}}=\dfrac{ku_{\mathrm{t}}\sin\psi_{\mathrm{e}}^{*}}{[1+(kz_{\mathrm{e}})^{2}]}+a_2+a_1r\\ \quad=u_{\mathrm{t}}f_1+a_2+a_1r\\ \dot{r}\ =a_3+\dfrac{T_r}{m_{33}}+\dfrac{d_r}{m_{33}}\end{cases} \tag{7}$$

where $f_1=k\sin\psi_{\mathrm{e}}^{*}/[1+(kz_{\mathrm{e}})^{2}]$.

From Eq. (6), we obtain

$$\psi_{\mathrm{e}}^{*}=w_{\mathrm{e}}-\arcsin\left(\frac{kz_{\mathrm{e}}}{\sqrt{1+(kz_{\mathrm{e}})^{2}}}\right) \tag{8}$$

We construct an equivalently nonlinear system for Eq. (7):

$$\begin{cases}\dot{\xi}_1=u_{\mathrm{t}}f_1+a_2+a_1\xi_2\\ \dot{\xi}_2=a_3+\dfrac{T_r}{m_{33}}+\dfrac{d_r}{m_{33}}\\ \dot{z}_{\mathrm{e}}=u_{\mathrm{t}}\sin\left(\xi_1-\arcsin\left(\dfrac{kz_{\mathrm{e}}}{\sqrt{1+(kz_{\mathrm{e}})^{2}}}\right)\right)\\ \zeta=\xi_1\end{cases} \tag{9}$$

where $\xi_1=w_{\mathrm{e}}$, $\xi_2=r$, and ζ denote system outputs. Note that the relative order of Eq. (9) is 2, and when the controller T_r renders the w_e (i.e., ξ_1) globally stable, the zero dynamics of Eq. (9) becomes

$$\dot{z}_{\mathrm{e}}=-ku_{\mathrm{t}}z_{\mathrm{e}}/\sqrt{1+(kz_{\mathrm{e}})^{2}} \tag{10}$$

Defining Lyapunov function as $V_z=z_{\mathrm{e}}^2/2$, and differentiating V_z along the solution of Eq. (9) yield $\dot{V}_z=-ku_{\mathrm{t}}z_{\mathrm{e}}^2/\sqrt{1+(kz_{\mathrm{e}})^{2}}\le 0$. By Lyapunov stability theorem [30], we can prove that z_{e} is globally asymptotically stable. Hence, Eq. (7) is a minimum phase and self-stabilization system. From Eq. (8), when w_{e} is globally converge to zero, we have

$$\psi_{\mathrm{e}}^{*}=-\arcsin\left(kz_{\mathrm{e}}/\sqrt{1+(kz_{\mathrm{e}})^{2}}\right) \tag{11}$$

where the global stability of z_{e} implies that the ψ_{e} is also globally asymptotically stable.

Based on the above analysis results, we obtain a conclusion. For Eq. (7), if we choose a feedback control law T_r to render w_e globally asymptotically stable, then guarantee that the original system state $(z_{\mathrm{e}},\psi_{\mathrm{e}}^{*})$ is globally asymptotically stable. Hence, system (Eq. (7)) is a minimum phase and self-stabilization system.

Note that the underactuated Eq. (7) has been simplified into a full-actuated system as follows:

$$\begin{cases}\dot{w}_{\mathrm{e}}=u_{\mathrm{t}}f_1+a_2+a_1r\\ \dot{r}=a_3+T_r/m_{33}+d_r/m_{33}\end{cases} \tag{12}$$

Obviously, the control problem of subsystem $(z_{\mathrm{e}},\psi_{\mathrm{e}}^{*},r)$ in underactuated Eq. (5) is transformed into the control of Eq. (12).

3.2 Backstepping adaptive dynamic sliding mode controller design

The controller design consists of two steps as follows.

Step 1: Stabilizing subsystem w_{e}.

Considering the following subsystem of Eq. (12)

$$\dot{w}_{\mathrm{e}}=u_{\mathrm{t}}f_1+a_2+a_1r \tag{13}$$

defining the Lyapunov function as

$$V_1=w_{\mathrm{e}}^2/2 \tag{14}$$

differentiating V_1 along the solution of Eq. (12) yields

$$\dot{V}_1=w_{\mathrm{e}}(u_tf_1+a_2+a_1r) \tag{15}$$

From Eq. (15), we choose the desired control input r as

$$\begin{aligned}r_{\mathrm{d}}&=-a_1^{-1}\cdot(u_{\mathrm{t}}f_1+a_2+k_1w_{\mathrm{e}})\\&=-\frac{m_{22}u_{\mathrm{t}}^2}{[m_{22}u_{\mathrm{t}}^2-m_{11}u^2]}\cdot\left[u_{\mathrm{t}}f_1-\frac{c(s)u_{\mathrm{t}}\cos\psi_{\mathrm{e}}^{*}}{1-c(s)z_{\mathrm{e}}}\cdot\right.\\&\qquad\left.k_1w_e-\frac{u}{u_t^2}\left(\frac{Y_\upsilon}{m_{22}}\upsilon+\frac{Y_{|\upsilon|\upsilon}}{m_{22}}|\upsilon|\upsilon\right)\right]\end{aligned} \tag{16}$$

where k_1 is a positive constant.

Remark 1: Note that Eq. (16) is singular when $1-c(s)z_{\mathrm{e}}=0$ or $m_{22}u_{\mathrm{t}}^2=m_{11}u^2$. However, Assumptions 1 and 2 imply that the conditions $1-c(s)z_{\mathrm{e}}>\lambda^{*}>0$ and $|m_{22}u_{\mathrm{t}}^2-m_{11}u^2|>0$ are simultaneously satisfied.

Substituting control law Eq. (16) into Eq. (15) yields

$$\dot{V}_1=-k_1w_{\mathrm{e}}^2\le 0 \tag{17}$$

However, r_d is not the actual control input; then we define the following error variable as

$$z_2 = r - r_d = r + a_1^{-1} \cdot (u_t f_1 + a_2 + k_1 w_e) \tag{18}$$

Substituting Eq. (18) into Eq. (15) yields

$$\dot{V}_1 = -k_1 w_e^2 + a_1 w_e z_2 \tag{19}$$

Clearly, Eq. (12) is rewritten as

$$\begin{cases} \dot{w}_e = -k_1 w_e + a_1 z_2 \\ \dot{z}_2 = a_3 - \dot{r}_d + \dfrac{T_r}{m_{33}} + \dfrac{d_r}{m_{33}} \end{cases} \tag{20}$$

Step 2: Stabilizing subsystem z_2.

Defining Lyapunov function as

$$V_2 = V_1 + z_2^2/2 + (d_r - \hat{d}_r)^2/(2m_{33}) \tag{21}$$

where $\hat{d}_r$ is the estimation value of uncertain impact d_r, and selecting the following switching function

$$S = c_1 z_2 + a_3 - \dot{r}_d + a_1 w_e + T_r/m_{33} + \hat{d}_r/m_{33} \tag{22}$$

where c_1 is a positive constant, from the second equation of Eqs. (20) and (22), we have

$$\dot{z}_2 = S - c_1 z_2 + (d_r - \hat{d}_r)/m_{33} - a_1 w_e \tag{23}$$

Differentiating V_2 along the solution of Eq. (20), and substituting Eq. (23) into it yield

$$\begin{aligned} \dot{V}_2 &= \dot{V}_1 + z_2 \dot{z}_2 - \dot{\hat{d}}_r (d_r - \hat{d}_r)/m_{33} \\ &= -k_1 w_e^2 + a_1 w_e z_2 - \dot{\hat{d}}_r (d_r - \hat{d}_r)/m_{33} + \\ &\quad z_2 \left[S - c_1 z_2 + (d_r - \hat{d}_r)/m_{33} - a_1 w_e \right] \\ &= -k_1 w_e^2 - c_1 z_2^2 + z_2 S + (z_2 - \dot{\hat{d}}_r)(d_r - \hat{d}_r)/m_{33} \end{aligned} \tag{24}$$

We define $\gamma = \dot{T}_r/m_{33}$, and make a time derivation of Eq. (22), then we have

$$\dot{S} = \gamma + c_1 \dot{z}_2 + \dot{a}_3 - \ddot{r}_d + \dot{\hat{d}}_r/m_{33} + a_1 \dot{w}_e + \dot{a}_1 w_e \tag{25}$$

Substituting the second equation of Eq. (20) into Eq. (25) yields

$$\begin{aligned} \dot{S} &= \gamma + c_1 (a_3 - \dot{r}_d + T_r/m_{33} + d_r/m_{33}) + \dot{a}_3 - \ddot{r}_d + \\ &\quad \dot{\hat{d}}_r/m_{33} + a_1 \dot{w}_e + \dot{a}_1 w_e \end{aligned} \tag{26}$$

Defining Lyapunov function as

$$V_3 = V_2 + S^2/2 \tag{27}$$

differentiating V_3 along the solutions of Eqs. (20) and (22), and substituting Eq. (26) into it yield

$$\begin{aligned} \dot{V}_3 &= \dot{V}_2 + S\dot{S} \\ &= -k_1 w_e^2 - c_1 z_2^2 + z_2 S + (z_2 - \dot{\hat{d}}_r)(d_r - \hat{d}_r)/m_{33} \\ &= -k_1 w_e^2 - c_1 z_2^2 + z_2 S + (z_2 - \dot{\hat{d}}_r)(d_r - \hat{d}_r)/m_{33} + \\ &\quad S \cdot [\gamma + c_1 (a_3 - \dot{r}_d + T_r/m_{33} + d_r/m_{33}) + \dot{a}_3] + \\ &\quad S \cdot [-\ddot{r}_d + \dot{\hat{d}}_r/m_{33} + a_1 \dot{w}_e + \dot{a}_1 w_e] \end{aligned} \tag{28}$$

We choose the following sliding mode arriving law

$$\dot{S} = -w_s S - k_s \operatorname{sgn}(S) \tag{29}$$

where k_s, w_s are positive constants; sgn(·) is a symbolic function. From Eq. (29), we choose the dynamical sliding mode control law γ as

$$\begin{aligned} \gamma = &-[c_1 (a_3 - \dot{r}_d + T_r/m_{33} + \hat{d}_r/m_{33}) + \dot{a}_3 - \ddot{r}_d] - \\ &[\dot{\hat{d}}_r/m_{33} + a_1 \dot{w}_e + \dot{a}_1 w_e + z_2 + w_s S + k_s \operatorname{sgn}(S)] \end{aligned} \tag{30}$$

Substituting Eq. (30) into Eq. (28) yields

$$\begin{aligned} \dot{V}_3 = &-k_1 w_e^2 - c_1 z_2^2 - w_s S^2 - k_s |S| + \\ &(z_2 + c_1 S - \dot{\hat{d}}_r)(d_r - \hat{d}_r)/m_{33} \end{aligned} \tag{31}$$

We design the adaptive law $\hat{d}_r$ as

$$\dot{\hat{d}}_r = z_2 + c_1 S \tag{32}$$

Substituting Eq. (32) into Eq. (31) yields

$$\dot{V}_3 = -k_1 w_e^2 - c_1 z_2^2 - w_s S^2 - k_s |S| \tag{33}$$

Therefore, if we select the suitably positive parameters k, k_1, c_1, k_s, w_s, the condition $\dot{V}_3 \le 0$ will be satisfied, namely, the control law (Eq. (30)) and adaptive law (Eq. (32)) make the state variables (w_e, z_2) of Eq. (20) globally asymptotically converge to zero. Hence, the subsystem (z_e, ψ_e^*, r) of Eq. (5) is also globally asymptotically stable.

3.3 Backstepping controller design

In this section, we consider the subsystem (z_e, ψ_e^*, r) of Eq. (5), and design a path following controller based on backstepping technique. We first assume the uncertain impacts as $d_\upsilon = 0$, $d_r = 0$.

Defining Lyapunov function as

$$V_4 = V_1 + z_2^2/2 \tag{34}$$

differentiating V_4 along the solution of Eq. (20), and substituting the second equation of Eq. (20) into it yield

$$\begin{aligned} \dot{V}_4 &= \dot{V}_1 + z_2 \dot{z}_2 \\ &= -k_1 w_e^2 + a_1 w_e z_2 + z_2 \cdot (a_3 - \dot{r}_d + T_r/m_{33}) \end{aligned} \tag{35}$$

To guarantee $\dot{V}_4 \le 0$, we design the feedback control law as

$$T_r = -m_{33}(a_3 - \dot{r}_d + k_2 z_2 + a_1 w_e) \tag{36}$$

where k_2 is a positive constant.

Substituting control law Eq. (36) into Eq. (35) yields

$$\dot{V}_4 = -k_1 w_e^2 - k_2 z_2^2 \le 0 \tag{37}$$

It is obvious that Eq. (20) is globally asymptotically stable with control law (Eq. (36)), and the subsystem (z_e,ψ_e^*,r) of Eq. (5) is also globally asymptotically stable. The stability analysis of closed-loop system is presented as follows.

3.4 Stability analysis

The stability analysis of Eq. (4) consists of two steps.

Step 1: Subsystem (z_e,ψ_e^*,r).

We can prove the stability of subsystem (z_e,ψ_e^*,r) by applying the design process of 3.2 section and 3.3 section.

Step 2: Subsystem υ.

When $z_e=0$, $\psi_e^*=0$, from the second equation of Eq. (4), we have

$$r=\left[\frac{m_{22}(u^2+\upsilon^2)}{m_{22}(u^2+\upsilon^2)-m_{11}u^2}\right]\cdot\left[c(s)\sqrt{u^2+\upsilon^2}+\frac{u}{(u^2+\upsilon^2)}\left(\frac{Y_\upsilon}{m_{22}}\upsilon+\frac{Y_{|\upsilon|\upsilon}}{m_{22}}|\upsilon|\upsilon-\frac{d_\upsilon}{m_{22}}\right)\right] \tag{38}$$

Substituting Eq. (38) into the third equation of Eq. (4) yields

$$\dot{\upsilon}=-\left[\frac{m_{22}(u^2+\upsilon^2)}{m_{22}(u^2+\upsilon^2)-m_{11}u^2}\right]\cdot\left(\frac{Y_\upsilon}{m_{22}}+\frac{Y_{|\upsilon|\upsilon}}{m_{22}}|\upsilon|\right)\cdot\upsilon+\left[\frac{m_{11}c(s)u(u^2+\upsilon^2)^{3/2}}{m_{11}u^2-m_{22}(u^2+\upsilon^2)}\right]+\left[\frac{m_{22}(u^2+\upsilon^2)}{m_{22}(u^2+\upsilon^2)-m_{11}u^2}\right]\cdot\frac{d_\upsilon}{m_{22}} \tag{39}$$

Defining Lyapunov function as

$$V_5=m_{22}\upsilon^2/2 \tag{40}$$

Differentiating V_5 along the solution of Eq. (4), and substituting Eq. (39) into it yield

$$\dot{V}_5=-\left[\frac{m_{22}(u^2+\upsilon^2)}{m_{22}(u^2+\upsilon^2)-m_{11}u^2}\right]\cdot(Y_\upsilon+Y_{|\upsilon|\upsilon}|\upsilon|)\cdot\upsilon^2+\left[\frac{m_{11}m_{22}c(s)u(u^2+\upsilon^2)^{3/2}}{m_{11}u^2-m_{22}(u^2+\upsilon^2)}\right]\cdot\upsilon+\left[\frac{m_{22}(u^2+\upsilon^2)}{m_{22}(u^2+\upsilon^2)-m_{11}u^2}\right]d_\upsilon\cdot\upsilon\le-\beta\upsilon^2+\mu|\upsilon| \tag{41}$$

where $\beta=\left[\frac{m_{22}(u^2+\upsilon^2)}{m_{22}(u^2+\upsilon^2)-m_{11}u^2}\right]\cdot(Y_\upsilon+Y_{|\upsilon|\upsilon}|\upsilon|)$, $\mu=\max\left(\left|\left[\frac{m_{11}m_{22}c(s)uu_t^3}{m_{11}u^2-m_{22}u_t^2}\right]+\left[\frac{m_{22}u_t^2}{m_{22}u_t^2-m_{11}u^2}\right]d_\upsilon\right|\right)$. From the **Assumption 2**, we can see that the expression $\left[\frac{m_{22}(u^2+\upsilon^2)}{m_{22}(u^2+\upsilon^2)-m_{11}u^2}\right]>0$, i.e., the parameter $\beta>0$. Eq. (41) is rewritten as

$$\dot{V}_5\le-\beta\upsilon^2/2,\quad\forall|\upsilon|>2\mu/\beta \tag{42}$$

According to the **Lemma 4.19** in Ref. [30], we can prove that the sway motion υ is input-to-state stable, and $\upsilon(t)$ satisfies

$$|\upsilon(t)|\le|\upsilon(t_0)|\mathrm{e}^{-\frac{1}{2}\beta(t-t_0)}+2\mu/\beta \tag{43}$$

where μ is a positive constant, the magnitude of constant μ is determined by uncertainty d_υ and curvature $c(s)$. Consider a special case: $d_\upsilon=0$, $c(s)=0$, then the constant $\mu=0$. Therefore, the sway motion υ is input-to-state stable.

Theorem 1: If we choose suitably positive parameters k, k_1, c_1, k_s, w_s, the control law (30) and adaptive law (32) can drive the subsystem (z_e,ψ_e^*,r) in system (Eq. (4)) globally asymptotically stable about the origin, and the sway motion υ is input-to-state stable.

Theorem 2: For Eq. (4), we assume the uncertainties $d_\upsilon=0$, $d_r=0$. If we choose suitably positive parameters k, k_1, k_2, the control law (Eq. (36)) can drives the subsystem (z_e,ψ_e^*,r) in Eq. (4) globally asymptotically stable about the origin, and the sway motion υ is input- to-state stable.

Proof: We can prove the **Theorems 1** and **2** based on the control design and stability analysis above.

4 Numerical simulations

In this section, we present some simulation tests on an USV [19] to verify the effectiveness of our proposed method. The nominal model parameters are given by $m_{11}^0=25.8$ kg, $m_{22}^0=33.8$ kg, $m_{33}^0=2.76$ kg·m^2, $X_u^0=12$ kg/s, $Y_\upsilon^0=17$ kg/s, $N_r^0=0.5$ kg·m^2/s, $X_{|u|u}^0=2.5$ kg/m, $Y_{|\upsilon|\upsilon}^0=4.5$ kg/m, $N_{|r|r}^0=0.1$ kg·m^2.

In the simulation, we pick the initial system states as: $x(0)=13$ m, $y(0)=0$, $\psi(0)=120°$, $u(0)=1$ m/s, $\upsilon(0)=0$, $r(0)=0$, namely, the center of expected path at the origin with radius R=10 m. Then, we can get the path following errors as $z_e(0)=-3$ m, $\psi_e^*(0)=30°$. We consider propeller input saturation conditions: $-2\ \mathrm{N\cdot m}\le T_r\le 2\ \mathrm{N\cdot m}$. The backstepping adaptive dynamical sliding mode controller is defined as BADSMC, and backstepping controller (BC) is defined as BC. We select the design parameters of BADSMC method as k=0.55, k_1=0.04, c_1=0.02, k_s=0.001, w_s=0.01, and BC method as k=0.55, k_1=0.04, k_2=20.

4.1 Simulation results of nominal model

We set the uncertain impacts as $d_u=d_\upsilon=d_r=0$ in the

simulation. The simulation results are shown in Figs. 2−4.

Figures 2 and 3 show that both controllers can force the USV following the desired path fast, i.e., to achieve the mission of path following with good manipulative performance. Figures 2 and 3 show that the position and state response curves of two controllers almost completely overlap. It is clear that both controllers have very similar convergence rate and dynamic performance under nominal model.

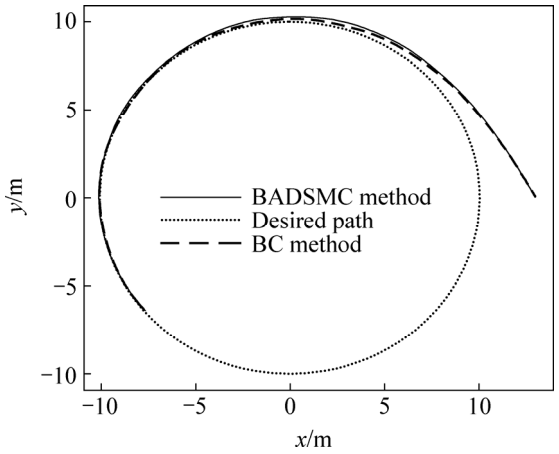

Fig. 2 Motion path of USV in nominal model

Figure 4 plots the response curves of control moment. For the case of BADSMC, we can see that the output of control moment is smooth without "chattering" phenomenon since the control information is indirectly generated by DSMC method of BADSMC. This can reduce the wear and energy consumption of propeller in actual operation, which is beneficial to the propeller. However, the BC directly obtains moment information so that the moment changes frequently.

4.2 Path following under uncertain influence

This section discusses the problem of path following with uncertainties to illustrate the performance and robustness of proposed method. We assume that the actual model has a parameter perturbation not more than 20%, without the loss of generality, consider an extreme situation in the simulation, and choose the following model parameters of actual USV: $m_{11}=0.9m_{11}^0$, $m_{22}=0.8m_{22}^0$, $m_{33}=0.8m_{33}^0$, $X_u=1.1X_u^0$, $Y_\upsilon=1.2Y_\upsilon^0$, $N_r=1.2N_r^0$, $X_{u|u}=0.9X_{|u|u}^0$, $\mathrm{Y}_{|\upsilon|\upsilon}=1.1\mathrm{Y}_{|\upsilon|\upsilon}^0$, $N_{|r|r}=1.1N_{|r|r}^0$.

From the nominal model simulation, we obtain that the maximums of sway and yaw accelerations are $\dot{\upsilon}_{\max}=0.015\ \mathrm{m/s^2}$, $\dot{r}_{\max}=2\ (°)/\mathrm{s^2}$. Therefore, we consider the following external disturbances with the same levels

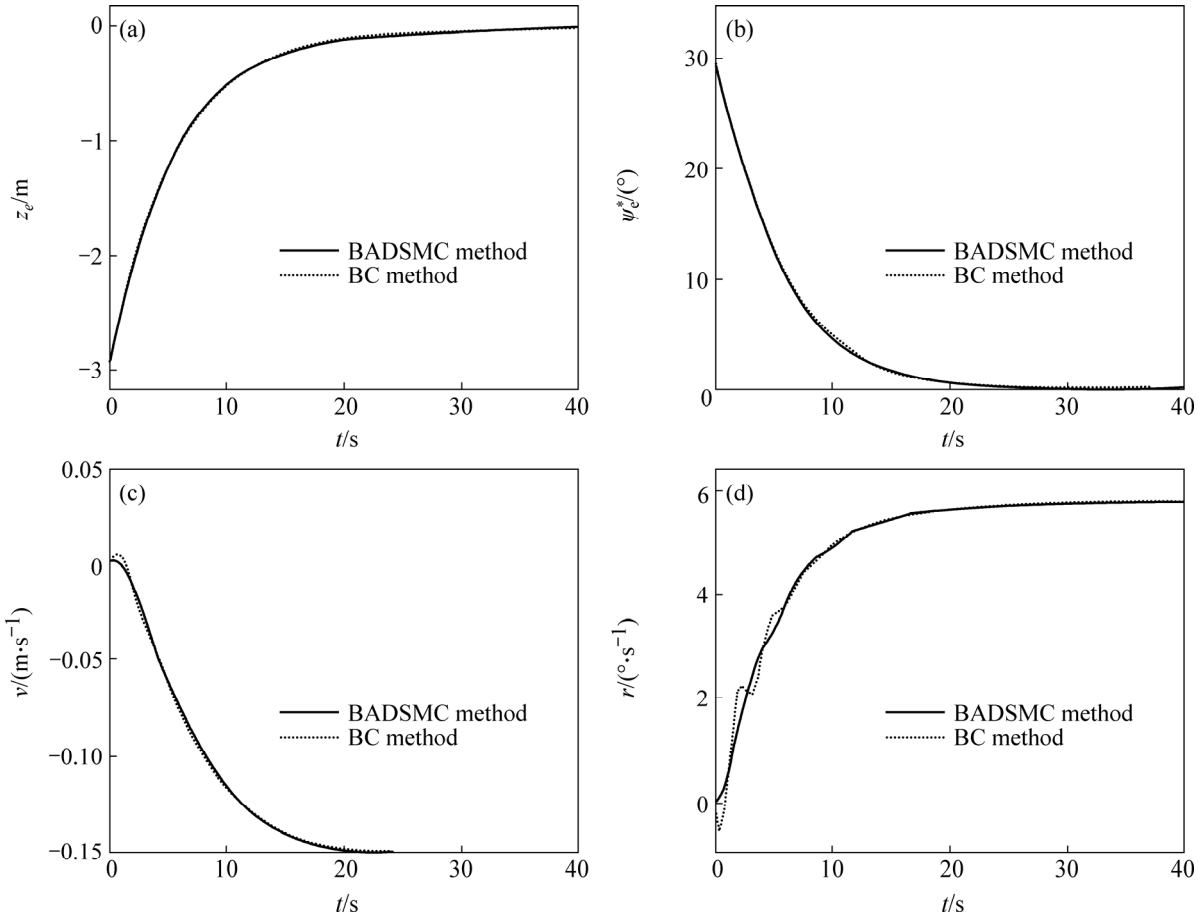

Fig. 3 Response curves of system state variables: (a) Distance between G and M; (b) Corrected cross-track error; (c) Sway velocity; (d) Yaw velocity

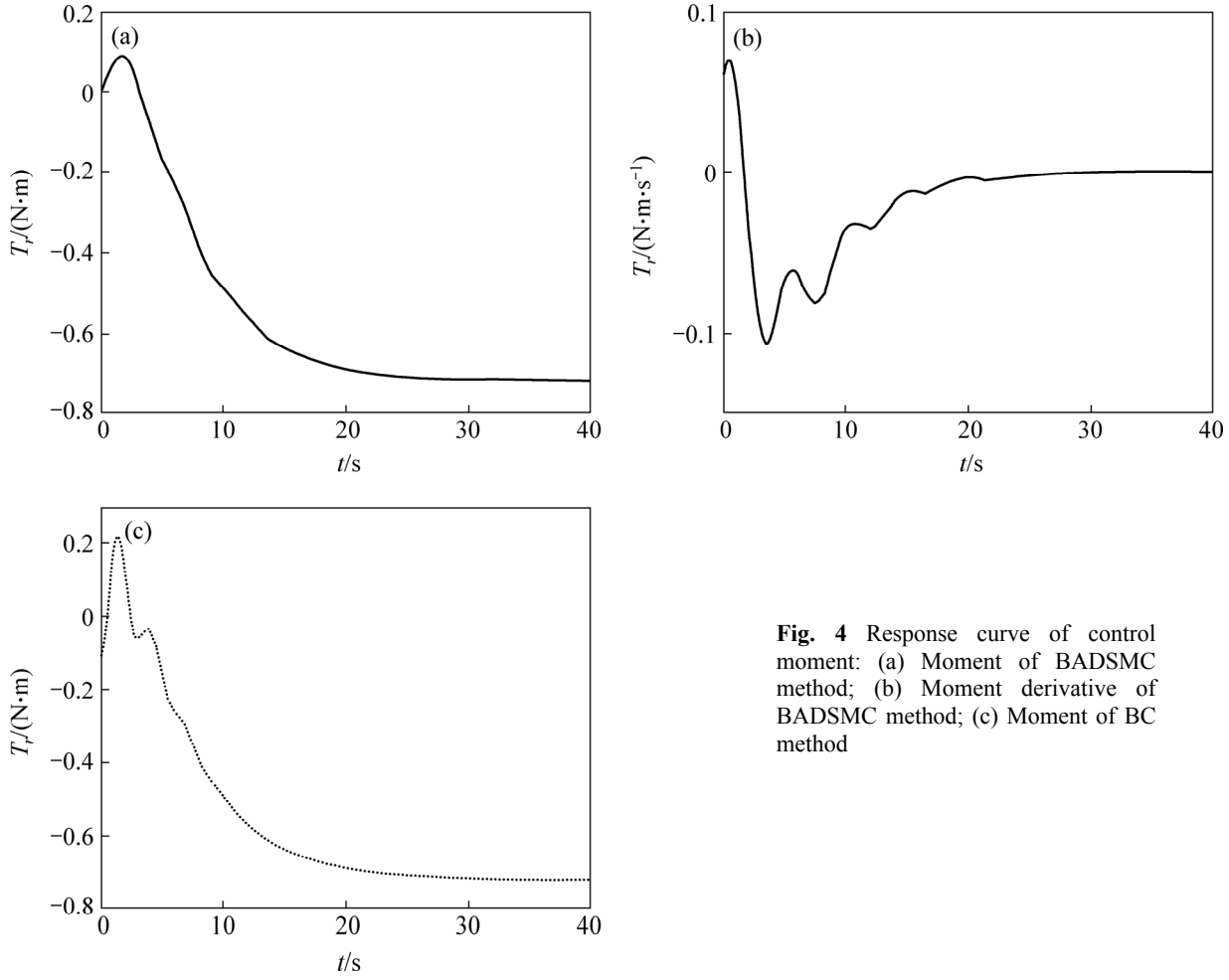

Fig. 4 Response curve of control moment: (a) Moment of BADSMC method; (b) Moment derivative of BADSMC method; (c) Moment of BC method

of $\dot{\upsilon}_{\max}$, $\dot{r}_{\max}$. $d_{\upsilon} = 0.01m_{22}^{0} \cdot [\sin(10\pi t) + \text{rand}(-1,1)]$, $d_{\text{r}} = 1.0m_{33}^{0} \cdot [\sin(10\pi t) + \text{rand}(-1,1)]$.

The simulation test is implemented under the uncertain influence, and the simulation results are given in Figs. 5−7.

Figures 5 and 6 show that the BADSMC guarantees the path-following errors $(z_{\text{e}}, \psi_{\text{e}}^{*})$ to quickly converge to zero, and the system output curves do not overshoot

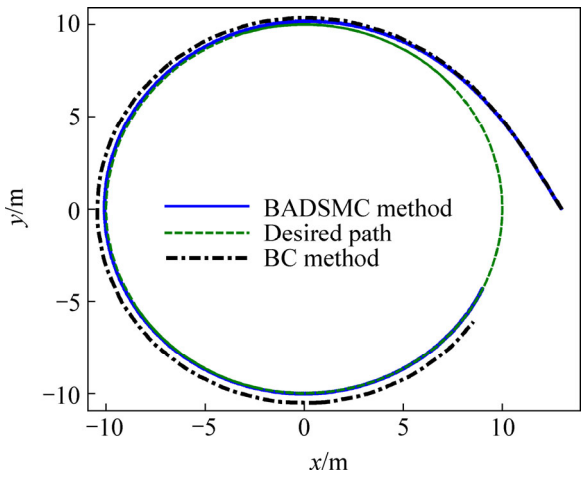

Fig. 5 Motion path of USV under uncertain influence

steady-state error. Although there are uncertainties, the BADSMC still completes the task of path following with uncertain impacts, namely, it has good ability to inhibit uncertain impacts.

However, by the BC method, the path following errors cannot converge to zero. The distance error z_{e} has some steady-state error, and the cross-track error ψ_{e} is oscillatory, thereby the USV cannot achieve the task of path following. Figure 6 shows that the velocity response curves are severely oscillatory, namely, the control effectiveness of BC is very poor due to uncertain influence. Figure 7 plots the response curves of control moment. The moment output fluctuation of BADSMC is smaller; while the moment output of BC has severe oscillation even moment saturation.

The above simulation results show that the BADSMC is insensitive to the model perturbation and external disturbance, and with good adaptive capacity and robust performance; while BC is more sensitive to the influence of uncertainty. It is obvious that the straight path following is a simple form of curvy path following; therefore, the proposed controller could be applied to solving the curvy and linear path following problem.

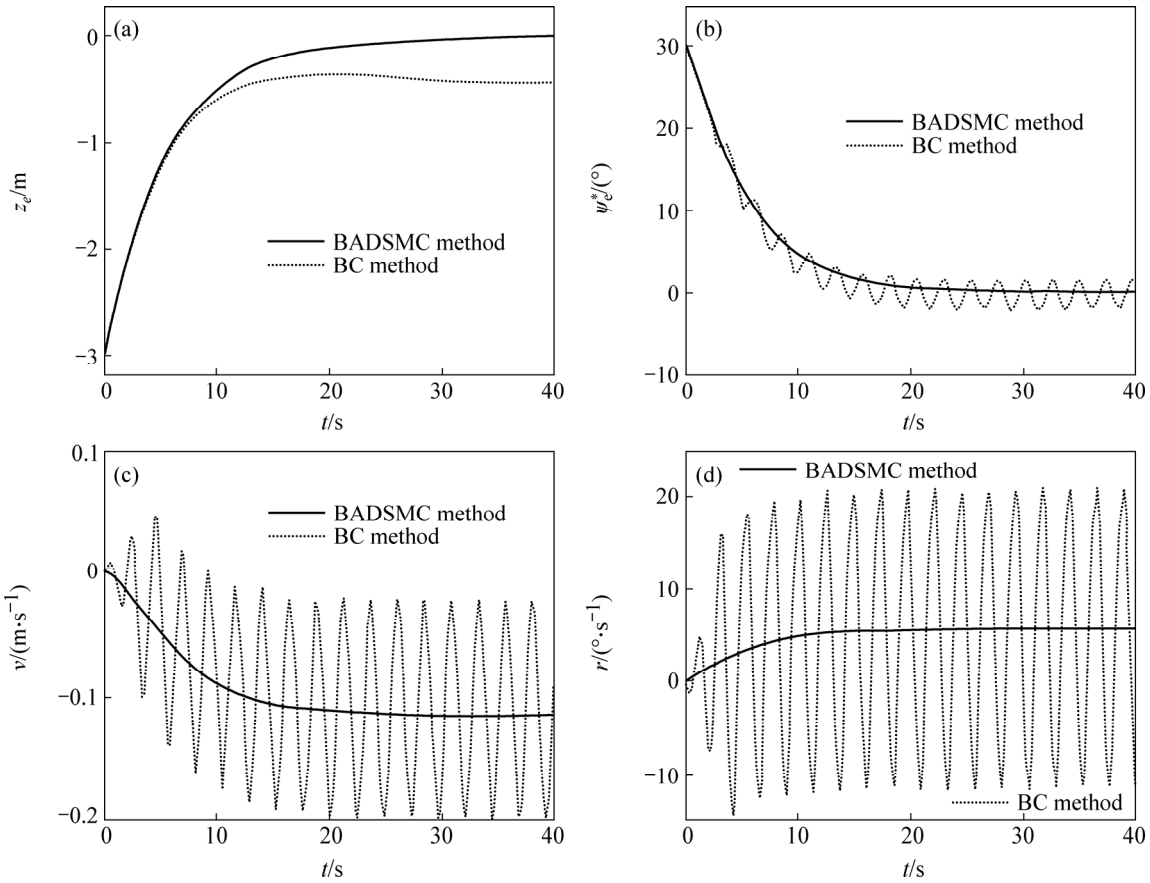

Fig. 6 Response curves of system state variables under uncertain influence: (a) Distance between G and M; (b) Corrected cross-track error; (c) Sway velocity; (d) Yaw velocity

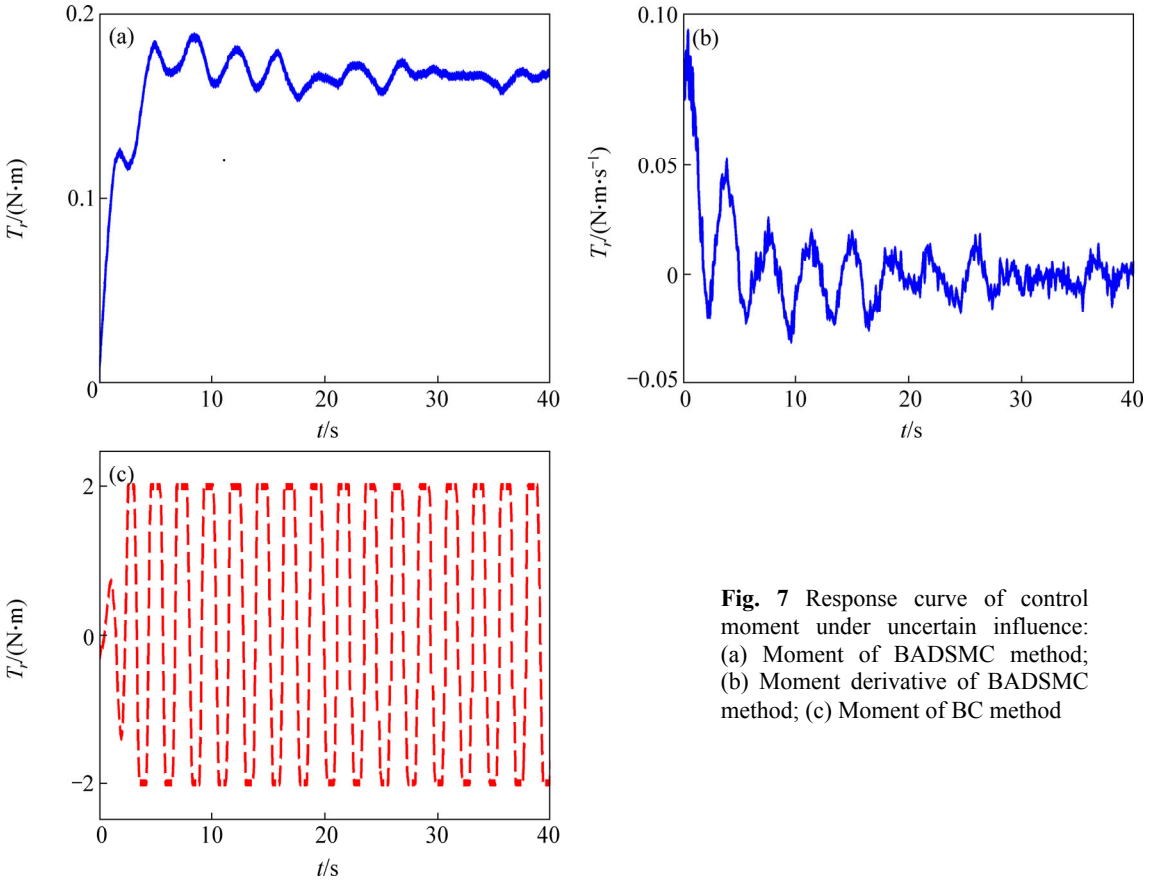

Fig. 7 Response curve of control moment under uncertain influence: (a) Moment of BADSMC method; (b) Moment derivative of BADSMC method; (c) Moment of BC method

5 Conclusions

1) The BADSMC method is proposed based on backstepping technique and theory of DSMC, and a BC method is designed via backstepping technique.

2) Theoretical analysis shows that both controllers can guarantee the subsystem (z_e, ψ_e^*, r) of original system globally asymptotically stable, and sway motion υ is input-to-state stable.

3) Simulation comparison tests reveal that compared with the backstepping controller, BADSMC method is insensitive to uncertainties, and has a better dynamic performance, adaptability and strong robustness. Moreover, the control output of BADSMC does not appear "chattering" phenomenon, namely, this method effectively weakens the "chattering" problem of sliding mode control. The theoretical analysis and simulation results validate the effectiveness of proposed method.

References

[1] KARIMI M, MOOSAVIAN S A A. Modified transpose effective jacobian law for control of underactuated manipulators [J]. Advanced Robotics, 2010, 24(4): 605−626.

[2] SANTHAKUMAR M, ASOKAN T. Investigations on the hybrid tracking control of an underactuated autonomous underwater robot [J]. Advanced Robotics, 2010, 24(11): 1529−1556.

[3] DO K D. Formation control of underactuated ships with elliptical shape approximation and limited communication ranges [J]. Automatica, 2012, 48(3): 1380−1388.

[4] DO K D, PAN J. Control of ships and underwater vehicles: Design for underactuated and nonlinear marine systems [M]. London: Springer, 2009: 12−158.

[5] DO K D, JIANG Z P, PAN J. Underactuated ship global tracking under relaxed conditions [J]. IEEE Transactions on Automatic Control, 2002, 47(9): 1529−1536.

[6] DO K D, JIANG Z P, PAN J. Robust adaptive path following of underactuated ships [J]. Automatica, 2004, 40(6): 929−944.

[7] LEFEBER E, PETTERSEN K Y, NIJMEIJER H. Tracking control of an underactuated ship [J]. IEEE Transactions on Control Systems Technology, 2003, 11(1): 52−61.

[8] BREIVIK M, FOSSEN T I. Path following for marine surface vessels [C]// Proceeding of the MTTS/IEEE TECHNO-OCEAN'04. Kobe, Japan: IEEE, 2004: 2282−2289.

[9] BREIVIK M, FOSSEN T I. Principles of guidance-based path following in 2D and 3D [C]// Proceeding of the 44th IEEE Conference on Decision and Control. Seville, Spain: IEEE, 2005: 627−634.

[10] LAPIERRE L, SOETANTO D, PASCOAL A. Nonlinear path following with applications to the control of autonomous underwater vehicles [C]// Proceeding of the 42nd IEEE Conference on Decision and Control. Hawaii, USA: IEEE, 2003: 1256−1261.

[11] ENCARNACAO P, PASCOAL A, ARCAK M. Path following for autonomous marine craft [C]// Proceedings of the 5th IFAC Conference on Maneuvering and Control of Marine Craft. Aalborg, Denmark: IFAC, 2000: 117−122.

[12] SKJETNE R, FOSSEN T I. Nonlinear maneuvering and control of ships [C]// Proceedings of the Ocean MTS/IEEE Conference and Exhibition. Honolulu, USA: IEEE, 2001: 1808−1815.

[13] DO K D, PAN J. State and output-feedback robust path-following controllers for underactuated ships using Serret-Frenet frame [J]. Ocean Engineering, 2004, 31: 587−613.

[14] LI Z, SUN J, OH S. Design, analysis and experimental validation of a robust nonlinear path following controller for marine surface vessels [J]. Automatica, 2009, 45: 1649−1658.

[15] AGUIAR A P, CREMEAN L, HESPANHA J P. Position tracking for a nonlinear underactuated hovercraft: controller design and experimental results [C]// Proceedings of the 42nd IEEE Conference on Decision and Control. Piscataway, NJ, USA: IEEE, 2003: 3858−3863.

[16] AGUIAR A P, HESPANHA J P. Trajectory-tracking and path-following of underactuated autonomous vehicles with parametric modeling uncertainty [J]. IEEE Transactions on Automatic Control, 2007, 52(8): 1362−1379.

[17] DO K D, PAN J. Globaltracking control of underactuatedships with nonzero off-diagonal terms in their system matrices [J]. Automatica, 2005, 41(9): 87−95.

[18] GHOMMAM J, MNIF F, BENALI A, DERBEL N. Nonsingular Serret-Frenet based path following control for an underactuated surface vessel [J]. Journal of Dynamic Systems, Measurement, and Control, 2009, 131(2): 1−8.

[19] DO K D, PAN J. Robust path-following of underactuated ships: Theory and experiments on a model ship [J]. Ocean Engineering, 2006, 33(10): 1354−1372.

[20] DO K D, PAN J. Global robust adaptive path following of underactuated ships [J]. Automatica, 2006, 42(10): 1713−1722.

[21] FOSSEN T I. Marine Control systems-guidance, navigation and control of ships, rigs and underwater vehicles [M]. Trondheim, Norway: Marine Cybernetics, 2002: 35−129.

[22] PETTERSEN K Y, LEFEBER E. Way-point tracking control of ships [C]// Proceedings of the 40th IEEE Conference on Decision and Control. Orlando, Florida, USA: IEEE, 2001: 940−945.

[23] KOSHKOUEI A J, BURNHAM K J. ZINOBER A S I. Dynamic sliding mode control design [J]. IEE Proceedings Control Theory Applications, 2005, 142(4): 392−396.

[24] DAVILA J, POZNYAK A. Dynamic sliding mode control design using attracting ellipsoid method [J]. Automatica, 2011, 47(1): 1467−1472.

[25] ANSARIFAR G R, DAVILU H, TALEBI H A. Gain scheduled dynamic sliding mode control for nuclear steam generators [J]. Progress in Nuclear Energy, 2011, 53(1): 651−663.

[26] SUNGSOO N, LEE B, CHOO J, MARZOCCA P. Robust dynamic sliding mode control of a rotating thin-walled composite blade [J]. Journal of Aerospace Engineering, 2011, 24(3): 298−308.

[27] WANG Z L, LIU Y H. Pose control of a lake surface cleaning robot using backstepping and polar coordinates [J]. Advanced Robotics, 2010, 24(4): 537−557.

[28] REFSNES J E, SRENSEN A J, PETTERSEN K Y. Model-based output feedback control of slender-body underactuated AUVs: Theory and experiments [J]. IEEE Transactions on Control Systems Technology, 2008, 16(5): 930−946.

[29] LIU Jin-kun, SUN Fu-chun. Research and development on theory and algorithms of sliding mode control [J]. Control Theory & Applications, 2007, 24(3): 407−418. (in Chinese)

[30] KHALIL H K. Nonlinear systems [M]. 3rd ed. Upper Saddle River, New Jersey, USA: Prentice-Hall, 2002: 124−238.

(Edited by YANG Hua)